

Review

Novel Development of Biocompatible Coatings for Bone Implants

Nicholas Yue Hou ¹, Hiran Perinpanayagam ¹, Mohammad Sayem Mozumder ² and Jesse Zhu ^{1,*}

¹ Department of Chemical and Biochemical Engineering, University of Western Ontario, London, ON N6A 5B9, Canada; E-Mails: nickh@live.com (N.Y.H.); hperinpa@uwo.ca (H.P.)

² Chemical & Petroleum Engineering Department, UAE University, Al-Ain P.O. Box 17555, United Arab Emirates; E-Mail: a.s.mozumder@uaeu.ac.ae

* Author to whom correspondence should be addressed; E-Mail: jzhu@uwo.ca; Tel.: +1-519-661-3807; Fax: +1-519-850-2441.

Academic Editor: James Kit-hon Tsoi

Received: 25 August 2015 / Accepted: 26 October 2015 / Published: 30 October 2015

Abstract: Prolonged life expectancy also results in an increased need for high-performance orthopedic implants. It has been shown that a compromised tissue-implant interface could lead to adverse immune-responses and even the dislodging of the implant. To overcome these obstacles, our research team has been seeking ways to decrease the risk of faulty tissue-implant interfaces by improving the biocompatibility and the osteo-inductivity of conventional orthopedic implants using ultrafine particle coatings. These particles were enriched with various bioactive additives prior to coating, and the coated biomaterial surfaces exhibited significantly increased biocompatibility and osteoinductivity. Physical assessments firstly confirmed the proper incorporation of the bioactive additives after examining their surface chemical composition. Then, *in vitro* assays demonstrated the biocompatibility and osteo-inductivity of the coated surfaces by studying the morphology of attached cells and their mineralization abilities. In addition, by quantifying the responses, activities and gene expressions, cellular evaluations confirmed the positive effects of these polymer based bioactive coatings. Consequently, the bioactive ultrafine polymer particles demonstrated their ability in improving the biocompatibility and osteo-inductivity of conventional orthopedic implants. As a result, our research team hope to apply this technology to the field of orthopedic implants by making them more effective medical devices through decreasing the risk of implant-induced immune responses and the loosening of the implant.

Keywords: ultrafine coating technology; bone implants; bioactive additives; biocompatibility; osteo-inductivity; calcium oxide; calcium phosphate

1. Introduction

Orthopedic and bone implants have achieved significant success in recent medical history due to their efficacy in enhancing or replacing damaged tissues. The material of choice for such implants is typically composed of commercially-available pure titanium or titanium alloy. Titanium proved to be an excellent candidate for bone implants because of its inert titanium dioxide layer that is formed once exposed to the atmosphere; this passive layer then essentially acts as a barrier between the implant and tissue, effectively preventing the implant from further oxidation, and consequently minimizing the chances of immuno-response. However, in addition to promoting biocompatibility, an ideal orthopedic implant would also need to ensure the appropriate integration of the implant into the patient's body in a process known as osteo-integration [1]. Only with sufficient levels of osteo-integration, the host can then provide proper anchorage to retain the implant, decreasing the chances for loosening of the implant and increasing its post-surgical success. Thus, much of the current research interest has been invested to improve the biocompatibility and the osteo-integration of orthopedic implants [2,3].

As a result, much effort has been dedicated to develop techniques that enrich the surface of biomaterial. For example, molecules such as hydroxyapatite ($\text{Ca}_{10}(\text{PO}_4)_6(\text{OH})_2$), calcium phosphate ($\text{Ca}_3(\text{PO}_4)_2$) and calcium oxide (CaO), as well as other arrays of mineral oxides were utilized to better mimic the bodily tissue [4–11]. Amongst the different minerals that were studied, researchers found that calcium is an especially beneficial surface-enriching molecule because it has been proven to be very osteo-inductive and is very effective at encouraging bone formation around the implants. Anitua *et al.* demonstrated that the incorporation of calcium ions onto the surfaces of biomaterials promoted near bone growth in rabbits' femora [12]. Similarly, other animal studies also confirmed the beneficial effects of calcium, such as improved bone formations in rat femora, increased healing of intrabony defects in dog mandibles, and enhanced resistance to dislodgement in rabbit tibia [13–15]. Furthermore, silica-calcium phosphate nano-composite coatings also showed improved alkaline phosphate activity of bone marrow stem cells that were attached onto the surfaces of biomaterials [16].

Since studies have demonstrated that the implant surfaces which mimic the bodily physiological environment exhibited the best potential for promoting desirable cellular responses, many approaches were proposed to be used for improving the performance of bone implants. These techniques included various forms of plasma spraying and sputter coating [17–20]. However, the surfaces created from these methods were often either too thick, lacked surface homogeneity, exhibited poor bonding strength, or the techniques were too expensive and time consuming for commercialization [21]. Thus, although research has shown promising results in improving the biocompatibility and osteo-integration of bone implants, more effective techniques are needed to incorporate mineral oxides onto the surface of biomaterials. To overcome this obstacle, we adopted our patented ultrafine particle coating technique. This technique allowed us to effectively construct highly-adherent, while thin, surface films to improve the biocompatibility and osteo-inductivity of bone implants.

Ultrafine powder coating has two major advantages over the conventional liquid solvent-based spray coating techniques, one of which is the environmental-friendliness achieved through the elimination of toxic solvents, while the other advantage is the economical-efficiency achieved from the ability to recycle over-sprayed particles. Nevertheless, the field of ultrafine powder coating has been saddled by one bane, the poor coating particle flowability. This phenomenon is caused by the decreasing particle size which resulted in the increasingly-dominating intermolecular forces, following by the aggregation of coating particles. To overcome this obstacle, our research group has developed a novel ultrafine particle technology where nano-additives were incorporated into the coating particles to act as spacers, thereby increasing the intermolecular distances and decreasing the intermolecular forces between the particles, consequently improving flowability and minimizing the aggregation of ultrafine coating particles [22,23]. Incorrect reference number, please rearrange. Similarly, based on this idea, our research team demonstrated that not only was our technology able to develop coat surfaces using ultrafine powder coating, but the utilization of functional additives also opened a realm which allows research to enrich surfaces with specific properties. During this study, we will discuss a collection of the uses of this technology along with functional additives for improving the biocompatibility and the osteo-inductivity of orthopedic implants [2,3,24–26].

During the coating of the titanium substrates, a polyester base-layer was created to act as a scaffold matrix for containing mineral additives. Various calcium-containing functional additive mixtures were then incorporated to the coating, forming a surface that promoted bone formation [27,28]. The functional additives consisted of only a small fraction of the surface coating particles to ensure the composition and integrity of the polyester [2,3]. Nevertheless, significant physical and biological differences were observed in cell cultures [2,3]. Over the last few years, we demonstrated that through this technique, we were able to construct uniform, continuous, homogenous, and highly adherent, as well as biocompatible, polymer coatings. Studies demonstrated that such surfaces also contained intricate nano-topographies and surface roughness, which were shown to enhance biocompatibility [3,25,26]. The culture used in our studies was a human embryonic palatal mesenchymal cell line (HEPM, ATCC CRL1486), derived from the developing palate of a human fetus. This cell line has provided us with a clinically-relevant model to study the cellular response to implant surfaces [29–31]. Our cellular studies demonstrated that the human mesenchymal cells attached, extended, proliferated, differentiated, and initiated biomineralization on the surfaces of modified biomaterials [2,3,24,25]. Through these studies, our research group hopes to use ultra-fine particle technology to develop more biocompatible and osteo-inductive biomaterial surfaces to improve the efficacy of orthopedic and bone implants.

2. Experimental Section

2.1. Sample Preparation

2.1.1. Bone Implants

In clinics, bone implants, typically composed of commercially-available pure titanium or titanium alloy, are anchored into the tissue through its screw-portion. As a result, the stability of the dental and many of the bone implants depends highly on the contact between the surface of the screw and the surrounding bones. To simulate such *in vivo* condition, the associating tissue-implant interface was

studied by coating one side of a titanium substrate using functionalized ultrafine particles, and HEPM cells were then seeded onto the enriched side.

2.1.2. Preparation of Ultrafine Coating Powder

This coating mixture is composed of mainly polyester resin (Avalanche White polyester, Links Coating, London, Ontario, Canada) and micron-sized TiO₂ (25 wt %) pigment. These particles were mixed and ground in a high-shear grinder to obtain ultrafine particles (<30 µm) that were then refined by passing through a sieve (35 µm). Nano-TiO₂ particles (0.5 wt %, Degussa, Parsippany, NJ, USA) were added to aid the flowability of such ultrafine particles, and bioactive functional additives, up to 5 wt % were added to ensure the integrity of the coating surface while still promoting biocompatibility and osteo-inductivity (Figure 1, Table 1). The coating mixture was then combined in the high-shear mixer and again passed through a sieve (35 µm) to obtain the final ultrafine coating particles.

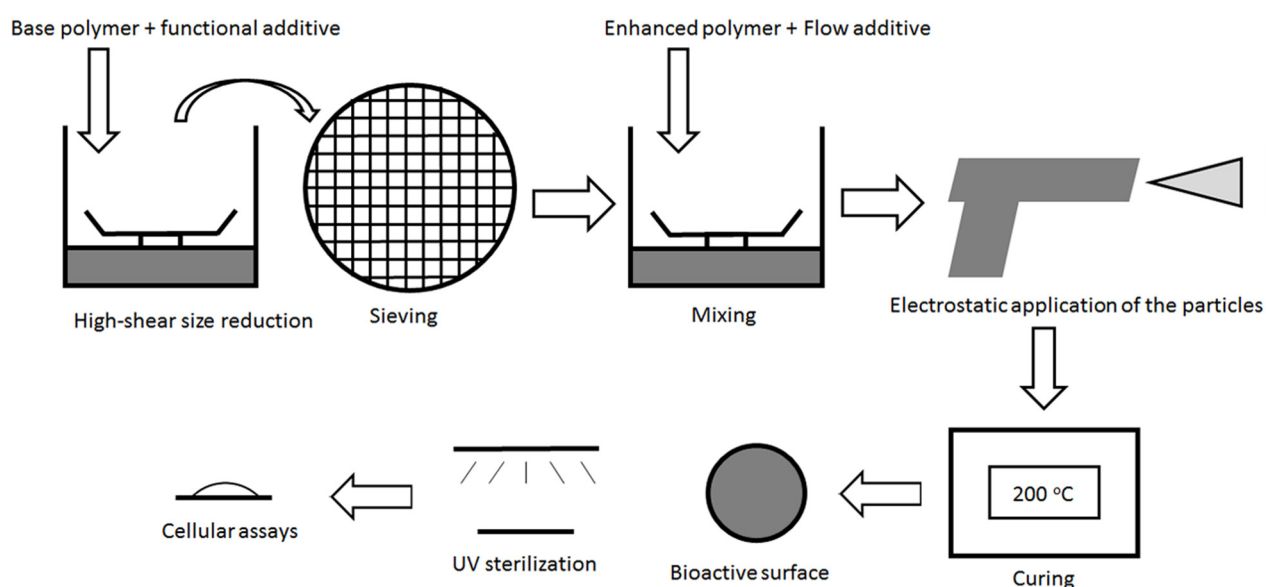


Figure 1. Ultrafine particle coating technology was utilized to construct these novel biocompatible, bioactive enriched surfaces. Here is a schematic illustration of the bioactive ultrafine particle coating process. The base polymer and the functional additive were sheared and sieved (35 µm) to obtain ultrafine particles; the sequential mixture was then mixed again with nano-sized titanium dioxide (nTiO₂) to improve this flowability. The surface enhancement particles were then electrostatically sprayed onto grounded titanium (CP-Ti) disks, cured in a furnace, and prepared for physical and biological examinations.

Table 1. An example of the enhancement particle formulation.

Coating	Base Polymer	Flow Additive (wt %)	Bioactive Agent (wt %)	Bioactive Calcium (mmol/100g)	Bioactive Phosphate (mmol/100g)
PPC (polymeric powder coating)			None	0.00	0.00
PPC + 1% CaO	Polyester resin	nTiO ₂ (0.5%)	CaO (1%)	17.83	0.00
PPC + 5% CaO			CaO (5%)	89.16	0.00
PPC + 5% CaP			Ca ₃ (PO ₄) ₂ (5%)	0.29	0.29

2.1.3. Powder Coating for the Modification of Biomaterial

The implant surfaces were modified using the ultrafine powder-coating technology. The ultrafine powders were sprayed onto commercially-available titanium substrates (CP-Ti, Grade 2, thickness = 0.5 mm, McMaster-Carr, Cleveland, OH, USA) (Figure 1). A Corona Gun (Nordson, Westlake, OH, USA) was used to apply a voltage (20 kV) which charged and sprayed the ultrafine particles onto grounded titanium substrates. Finally, the thin layer of particles on the titanium substrate were cured in a high performance air flow oven (200 °C, 10 min, Sheldon manufacturing, Inc., Cornelius, OR, USA). The coated titanium substrates were then cut into circular disks (diameter = 24 mm) for further analysis.

2.2. Physical Characterizations

2.2.1. Particle Size Analysis

Particle size analysis was conducted to ensure the ultrafine characterization of the coating powders. The dimensions of these ultrafine powders were examined using a BT-9300s Laser Particle Analyzer (Ningbo Yinzhou Hybers, Ningbo, China). The powders were suspended in water and a laser stream was used to create a diffraction pattern that was then reflected onto a detector and analyzed to measure the particle size distribution. Through laser analysis, the results confirmed the ultrafine classification of the coating powders by exhibiting a D50 of less than 30 μm (Figure 2).

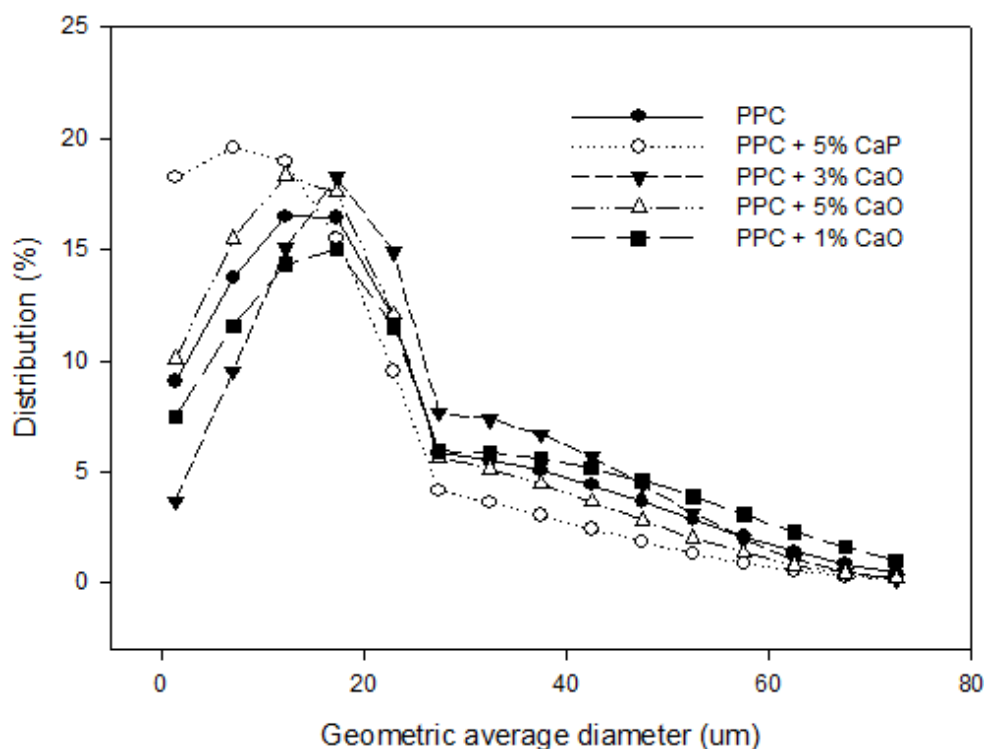


Figure 2. Size distribution of the various bioactive surface coating particles. Laser particle analysis indicated that all of the particle mixtures constructed using the ultrafine particle technology had a D50 of less than 35 μm , confirming the ultrafine nature of the particles. In addition, all of the coating particles exhibited a similar size distribution, illustrating the reliability of the ultrafine particle technology.

2.2.2. Surface Analysis

The modified biomaterial surfaces were characterized for their surface composition and homogeneity as previously described [6]. The surfaces were analyzed using energy dispersive X-ray spectroscopy (EDX) with a Hitachi S-4000 scanning electron microscope (SEM) (Hitachi, Pleasanton, CA, USA). The coated biomaterials were mounted onto metal stubs, secured by adhesive carbon tape and coated with a 10 nm thick gold film. The working voltage and working distance of the SEM were respectively set at 15 kV and 15 mm. Sequentially, each element was identified (minimum detection limit = 0.01%) and its presence was calculated (wt %). The EDX analyses were repeated at three separate locations on each surface, and the mean concentrations of the key elements were then calculated. Additionally, the EDX analyses were repeated across the entire surface of each disk to identify the presence and distribution of the key elements, providing an elemental mapping of key elements.

2.2.3. Hydrophilicity Assay

The different biomaterial surfaces were compared for their wettability through measuring their water contact angles. Water droplets (80 μL) were dripped onto each surface, and their water contact angles were measured using a Ramé-Hart Model 100 goniometer (Ramé-Hart Instrument Co., Succasunna, NJ, USA). These measures were repeated five times to ensure reproducibility.

2.2.4. Surface Roughness Analysis

Surface roughness, which has been suggested to improve the cell attachment onto biomaterial, were analyzed with a dynamic force mode XE-100 atomic force microscope (AFM) (Park Systems, Suwon, Korea). The spring cantilever had a length of 125 μm , a width of 40 μm and a thickness of 4 μm . The spring constant was $\sim 40 \text{ N}\cdot\text{m}^{-1}$ and the nominal tip radius of the silicon cantilever was 10 nm. The biomaterials were examined at room temperature, and 256×256 pixel resolution images were recorded. These images were analyzed with image processing and analysis software (XEI 1.7, Park Systems, Suwon, Korea) to demonstrate the roughness of each individual surface.

2.3. Biocompatibility

2.3.1. Protein Localization and Visualization

The localization of actin filaments and the intracellular features of mesenchymal stem cells were visualized using immunocytochemistry. Human embryonic palatal mesenchymal cells (HEPMs, ATCC CRL-1486) were seeded onto coated and titanium control discs which were held in 24-well tissue culture plates (50,000 cells/well). The cultures were maintained in Dulbecco's Modified Eagles Medium (DMEM) supplemented with fetal bovine serum (FBS, 10%), L-glutamine ($2 \mu\text{mol}\cdot\text{mL}^{-1}$), penicillin G ($100 \text{ U}\cdot\text{mL}^{-1}$), streptomycin sulfate ($100 \mu\text{g}\cdot\text{mL}^{-1}$), and amphotericin B ($0.25 \mu\text{g}\cdot\text{mL}^{-1}$) at 37°C within an incubator. After 24 h, the surfaces were harvested and washed three times using phosphate buffered saline (PBS). The cells that were attached to the surfaces were fixed in paraformaldehyde (4% for 10 min) and permeabilized by Triton X-100 (0.1% for 5 min). The actin filaments of the cytoskeleton were labelled (stained for 2 h) with rhodamine phalloidin (Cytoskeleton, Denver, CO, USA).

The surfaces were then mounted using Vectashield with DAPI (Vector Laboratories, Burlingame, CA, USA) and sequentially examined by an inverted fluorescence microscope (Axiovert 40 CFL, Carl Zeiss Canada Ltd, Toronto, ON, Canada).

2.3.2. Optical and Scanning Electron Microscopy

Cell morphology can often reveal information regarding the biocompatibility of the surface; thus, optical and scanning electron microscopes (SEM) were utilized to examine the morphologies of the HEPM cells raised on the various biomaterials. After 24 h of incubation, the biomaterials were removed from the incubator and rinsed three times in PBS. Cells that remained attached to the disks were fixed in paraformaldehyde (4% PFA, Fisher Scientific, Hampton, NH, USA) for 24 h at room temperature. The disk surfaces were then examined using an optical microscope at 100× and 400× magnification.

In addition, cellular morphologies and cell-surface interactions were visualized in greater details using SEM. After 24 h of cell attachment and spreading, the surfaces were collected and washed three times using PBS. They were then fixed with glutaraldehyde (2.5% for 20 min) in cacodylate buffer (100 mM), dehydrated in ascending grades of ethanol (25%, 50%, 75%, 95%, and 100%) and immersed in hexamethyldisilazane. Lastly, the surfaces were air dried, mounted on metal stubs, sputtered with nano-sized gold particles (20 nm) and examined with a Hitachi S-2600 SEM (Hitachi, Pleasanton, CA, USA).

2.4. Mineralization Assays

The surfaces of biomaterials were assessed for their capacity to induce the osteogenic differentiation and the biomineralization of attached cell cultures. Biomaterials seeded with HEPM cells were incubated in culture media. After the initial 24 h period, DMEM were replaced with enriched media containing ascorbic acid (50 $\mu\text{mol/mL}$) and β -glycerophosphate (10 $\mu\text{mol/mL}$) as additives to induce osteogenic differentiation. The osteogenic media was replenished every three days throughout the assay and the cultures were maintained for either two or four weeks.

Following the two and four week periods of differentiation, the culture media were discarded and the cell cultures were gently rinsed in PBS and fixed in formalin (4%) for 1 h. They were then rinsed twice in calcium-free Nanopure water and stained with Alizarin Red-S (2%, EMD) for 10 min at room temperature. Lastly, the surfaces were examined for stained mineral deposits and images were captured digitally.

2.5. Cellular Assays

2.5.1. Cell Proliferation Assay

The ability of the coated biomaterials in improving cellular attachment and proliferation were quantified by hemocytometry assays. Human mesenchymal cells were seeded onto various surfaces in 24-well tissue culture plates (50,000 cells/well). After 24 and 72 h of cell attachment and proliferation, the biomaterials were transferred to a different 24-well tissue culture plates and triplicate cultures were analyzed for each surface. These cultures were rinsed with PBS to remove unattached cells, trypsin (150 μL) was then added to each well and the culture plates were incubated (37 °C for 5 min) to release the attached cells. These cells were then collected and analyzed using a hemocytometer.

2.5.2. Metabolic Activity

The metabolic activity of the cells raised on various surfaces were measured using MTT assay. After 24 and 72 h of attachment and proliferation, the surfaces were rinsed with trypsin to release the attached culture. These cells were then collected and reseeded into multiple 48-well tissue culture plates. After 24 h, MTT reagent (tetrazolium (3-(4,5-dimethylthiazolyl)-2)-2, 5-diphenyltetrazolium bromide) was added to each cultures before they were incubated (37 °C) for an hour in the dark. The reagents were then replaced with an MTT solubilizing solution (acid-isopropanol), and the colorimetric absorbance were measured (570 nm) in a Safire Multi-Detection Microplate Reader (Tecan, San Francisco, CA, USA).

2.5.3. Gene Expression

The attached cells were analyzed for their expression of osteogenic differentiation marker genes through RT-PCR analysis. During this assay, HEPM cells (200,000 cells/well) were first seeded onto replicate of biomaterial surfaces in six-well tissue culture plates. After 24 h, ascorbic acid (50 $\mu\text{mol}\cdot\text{mL}^{-1}$) and β -glycerophosphate (10 $\mu\text{mol}\cdot\text{mL}^{-1}$) were added to the media to induce osteogenic differentiation.

After incubating in osteogenic media, cell cultures were harvested to analyze their gene expression. The cultures were rinsed three times with PBS to remove unattached cells, the cellular RNA was then extracted with an RNeasy Mini kit (Qiagen, Valencia, CA, USA) according to the manufacturer's instructions. Sequentially, the cells were re-suspended in lysis buffer and homogenized by passage through a QIA shredder column (Qiagen, Hilden, Germany). The homogenized lysate was then applied to the RNeasy column, rinsed repeatedly with a series of buffers (RLT), and eluted into RNase-free deionized water. These RNA extracts were kept at -70 °C for storage. Following the dilution of aliquots in deionized water, RNA extracts were examined using a bioanalyzer (Agilent Technologies, Wilmington, DE, USA) to measure gene expression using PCR.

During analysis, RNA extracts were subjected to conventional RT-PCR Analysis with human-specific primers for Runt-related transcription factor 2 (RUNX2), type I collagen (COL1A1), alkaline phosphatase (ALP), bone sialoprotein (BSP), and glyceraldehyde 3-phosphate dehydrogenase (GAPDH), as reported in previous studies [32]. The RNA was reverse transcribed into cDNA with Oligo (DT) primer and SuperScript TM II RNase H Reverse Transcriptase at 42 °C for 50 min. The specific transcripts were then amplified in separate tubes using PCR with gene-specific primers and Platinum R© Taq DNA polymerase. The thermal cycling parameters were set at 94 °C for 2 min to activate the polymerase, followed by 40 cycles of 94 °C for 30 s, 50 °C for 30 s, and 72 °C for 1 min. The RT and PCR reactions were performed in an AmpliTronR© II thermocycler (Barnstead Thermolyne, Dubuque, IA, USA). The PCR products were separated on an agarose gel (1%) containing ethidium bromide (0.05 $\mu\text{g}\cdot\text{mL}^{-1}$), visualized on a trans-illuminator (Fisher, Pittsburgh, PA, USA) and recorded digitally (Panasonic, Osaka, Japan).

3. Results and Discussion

3.1. Biocompatible Surface Coating

After the incorporation of bioactive functional additives using ultrafine powder coating, our research team has demonstrated that this technology could be successfully utilized to improve the biocompatibility and osteo-inductivity of titanium-based orthopedic and dental implants. Bone implants are typically composed of titanium and its alloys due to the inert passive titanium dioxide. This insulating layer significantly reduced the chances of inflammation due to the oxidation of implant material. However, the success of orthopedic implants is also heavily dependent on a process known as osteo-integration. Previous studies have suggested that osteo-integration can be affected by various characteristics of the implant surface, such as its surface roughness, hydrophilicity, and surface chemical composition [13,33–37].

It was postulated that the ultrafine particle technology can be used to incorporate various bioactive mineral additives onto the surface of implant substrate, thereby improving the biocompatibility and the osteo-inductivity of bone implants. This technology relies on the use of nano-flow additives to reduce the aggregation of ultrafine particles, and the incorporation of bioactive-functional additives to enhance the biocompatibility and the osteo-inductivity of bone implants. Only a maximum of 5 wt % of bioactive additive was added to ensure the integrity of the resultant coated surface. Prior to the application of the surface enhancement particles, particle size analysis was conducted to ensure the ultrafine characteristic of the coating particles. After coating, the resultant biomaterials were then assessed for their physical characteristics, biological performances, as well as cellular responses for their efficacy to determine the best potential surface coating formulation for enhancing bone implants.

3.2. Physical Characterizations

After the implant substrates were coated, the resultant surfaces were further studied and compared for their physical characteristics. The coated biomaterials were examined for their surface composition using EDX. The results demonstrated that the majority of the surface coating was composed of carbon and oxygen, which complied with the chemical composition of polyester. EDX also revealed that by varying the bio-additives, the sequential changes in the chemical composition were readily detected. Specifically, the EDX results demonstrated that the presence of calcium increased with the proposed enrichment formulation (Figure 3). Similarly, specific elements were only detected in their respective designated formulation groups, such as phosphorous was only detected in calcium phosphate-coated surfaces. These findings demonstrated that the surfaces were accurately coated according to our anticipation and mineral formulation, and the reliability of the ultrafine coating technology.

Sequentially, elemental mapping was utilized to examine the localization and the distribution of bioactive functional additives (Figure 4). Like EDX, the results suggested that calcium and phosphorus, two different components of the bioactive additives, were absent in the titanium and polyester control surfaces and the presence of calcium also increased with its formulation. In addition, calcium was also found to be co-localized with phosphorus in calcium phosphate-enriched surfaces, indicating that the electrostatic spraying process can safely maintain the integrity of the functional additives, and demonstrating the non-destructive quality of the powder application technique. Together with EDX and

elemental mapping, the reliability of the ultrafine-particle coating technique to accurately enrich titanium surfaces was confirmed.

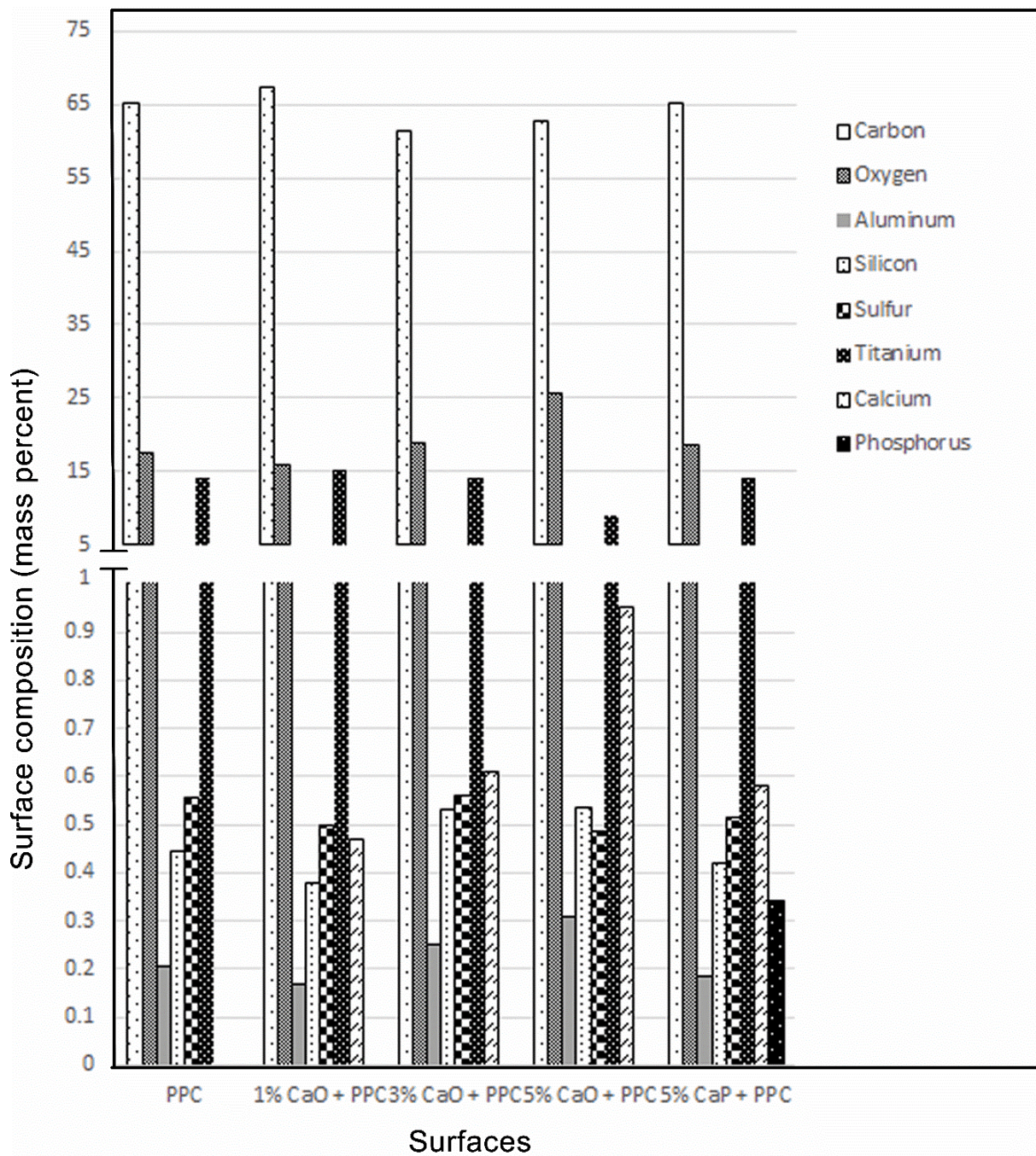


Figure 3. EDX was used to detect the presence of various elements on coated surfaces. This analysis demonstrated that the surface coating particles were composed mostly out of carbon, oxygen, and titanium. However, there are smaller quantities of aluminum, silicon, and sulfur that came from the polymer backbone. In addition, the calcium presence increased with the increasing incorporation of calcium oxide, and phosphors were only detected in calcium phosphate-containing mixtures. Collectively, these findings confirmed the accuracy of the ultrafine particle technology in incorporation functional additives.

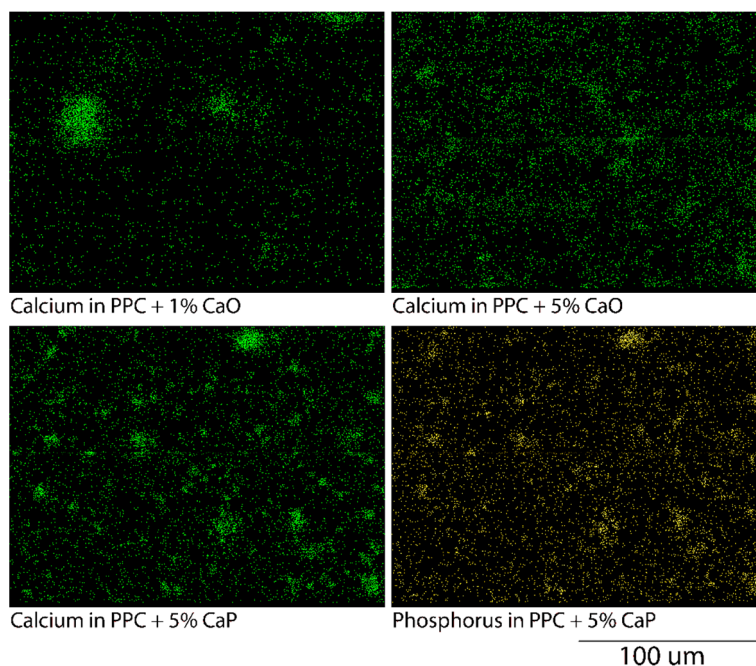


Figure 4. Elemental mapping of calcium and phosphorus on the different coated surfaces. These images illustrated that calcium existed in smaller clusters while under low concentration, whereas it is more evenly spread out at higher concentration. In addition, element mapping also demonstrated that the phosphorus was co-localized with calcium in calcium phosphate surfaces. (Adapted and modified from [2]).

Moreover, previous studies have suggested that the biocompatibility of a bone implant surface depends highly on its hydrophilicity; thus, the water-wettability of enriched biomaterials was compared to the conventional titanium substrate to assess their potential biocompatibility. The hydrophilicity of each surface was examined by measuring the water contact angle using a goniometer. Although all of the surfaces were hydrophilic, the results suggested that the commercially-pure titanium exhibited the highest hydrophilicity, followed by 5% calcium oxide-containing surfaces, whereas the polymer-control and the calcium phosphate-enriched surfaces were found to be the most hydrophobic (Figure 5). More interestingly, the results also illustrated a correlation between the hydrophilicity and the quantity of incorporated calcium oxide. The outstanding hydrophilicity demonstrated by the titanium control substrate could be the result of the passive titanium dioxide layer that was formed on the surface, which increased the polarity of the surface and its ability in attracting water. However, the weaker water-wettability exhibited by the polymer control surfaces could be the consequence of the extensive presence of carbon, a very neutral element. Nevertheless all of the surfaces were expected to be biocompatible due to their hydrophilicity.

In addition to hydrophilicity, surface roughness has been shown to aid cell attachment and improve biocompatibility. Thus, the surface roughness of the enriched biomaterials were also compared to the commercially available titanium substrate. Through AFM, not only the enriched surfaces demonstrated a greater surface roughness at a micron level, but a series of complex and intricate convexities and concavities were also noted on enriched surfaces when examined at a nano-level (Figure 6). These findings suggested that the surface coating could improve the attachment of tissue cells by increasing the surface roughness and, consequently, increasing the biocompatibility of the biomaterial [32,34,38].

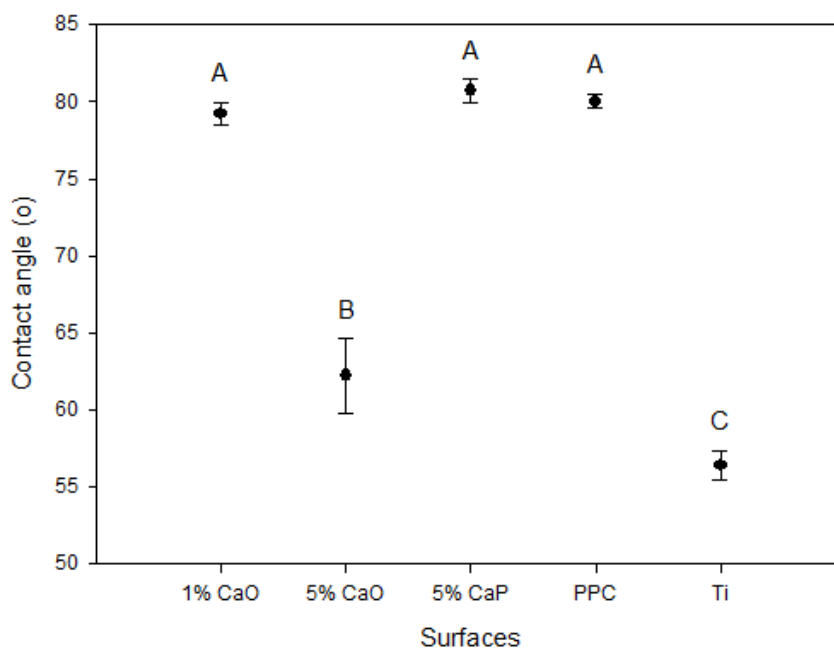


Figure 5. Water wettability assay of the different biomaterial surfaces. The hydrophilicity assay indicated that by increasing the percent of surface calcium oxide, its hydrophilicity can be significantly increased. Furthermore, although all of the surfaces were hydrophilic, the 5% calcium oxide and the conventional titanium surfaces were significantly more hydrophilic than rest of the biomaterials. Each alphabet represents an individual statistical group. (One way ANOVA, $p > 0.05$).

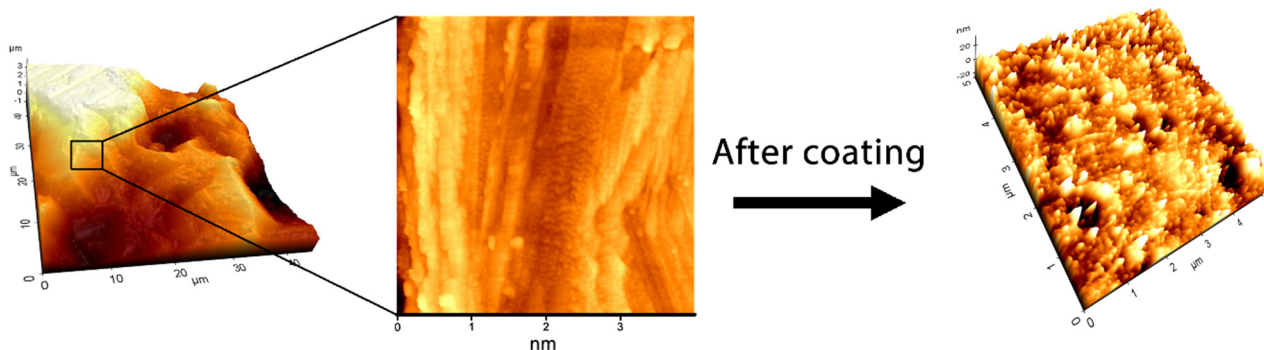


Figure 6. Atomic force microscopy (AFM) was employed to demonstrate the change in biomaterial surface roughness before and after coating. The images showed the smooth surface of the conventional titanium substrate; however, after polymeric coating, intricate nano-sized topographies can be observed on the surface of the biomaterial.

In conclusion, physical assessments demonstrated that, in addition to reliably producing ultrafine coating particles, the ultrafine-particle technology can also be used to accurately coat commercially-available titanium substrates. Furthermore, the coated surfaces were also found to be hydrophilic and contained complicated surface topographies which could aid in cellular attachment and improve the biocompatibility of such surfaces.

3.3. Biocompatibility

In order to obtain a more in-depth and relevant information regarding the biological performance of ultrafine particle coated surfaces, the bioactivity of cells that were raised on such coated surfaces were examined to assess their biocompatibility and osteo-inductivity. The extent of such two qualities were studied by conducting an array of biological *in vitro* assays which examined the cell morphology and biomineralization activities.

Using immunochemistry, the nuclei of attached cells were stained using 4',6-diamidino-2-phenylindole (DAPI) and the actin filaments were labeled with phalloidin (Figure 7). The fluorescent microscopy images illustrated that the cell existed in clustered cultures, suggesting attachment of HEPM cells and their high cellular density; the phalloidin staining demonstrated the extended morphology, which is often correlated with intimate cell-surface associations as a result of the biocompatibility of the surface [33].

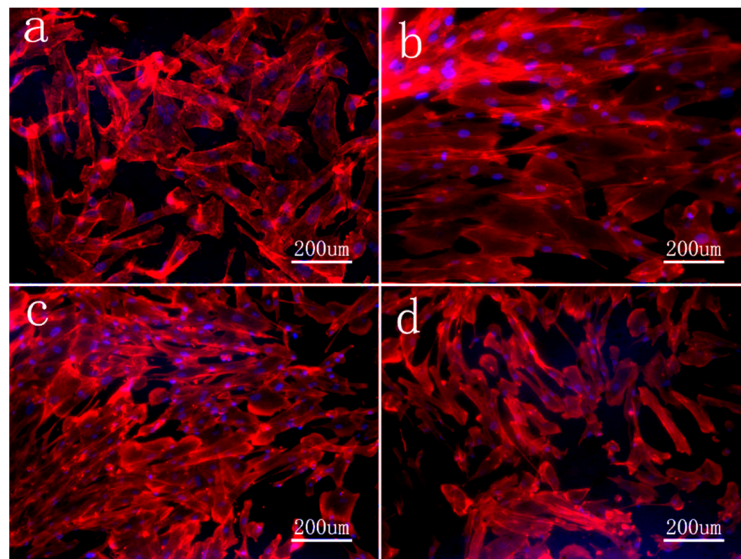


Figure 7. Immunochemistry of the cytoskeletal integrity of attached cells examined using a fluorescent microscope. The different figures illustrated the similar culture density and morphology of the cells that were raised on coated titanium substrate, demonstrating the consistency in performance of enriched biomaterial. In addition, immunochemistry showed the very organized actin filaments in all of the cells, and their stretch morphology. (a) Conventional titanium substrate, (b) PPC-4, (c) PPC-5, (d) PPC-6, according to Table 2.

The associations between the biomaterial and the cellular morphology were further studied using optical and high-resolution scanning electron microscopes (SEM). SEM images illustrated that all of the surfaces were able to support cells, all of which exhibited a spreading morphology, suggesting their biocompatibility (Figure 8). Moreover, the microscopy images also demonstrated cell clusters and the close association between cell cultures and the underlying biomaterial, again confirming the biocompatibility of enriched titanium surfaces. Furthermore, optical microscopy also suggested that the cellular confluency of the biomaterial was increased with the increasing incorporation of calcium oxide, resulting in the highest cellular confluency in 5% CaO surfaces, whereas the commercially-pure titanium exhibited the least amount of cell confluency (Figure 9). In other words, the increase in the incorporation of CaO also increased the biocompatibility of coated biomaterial.

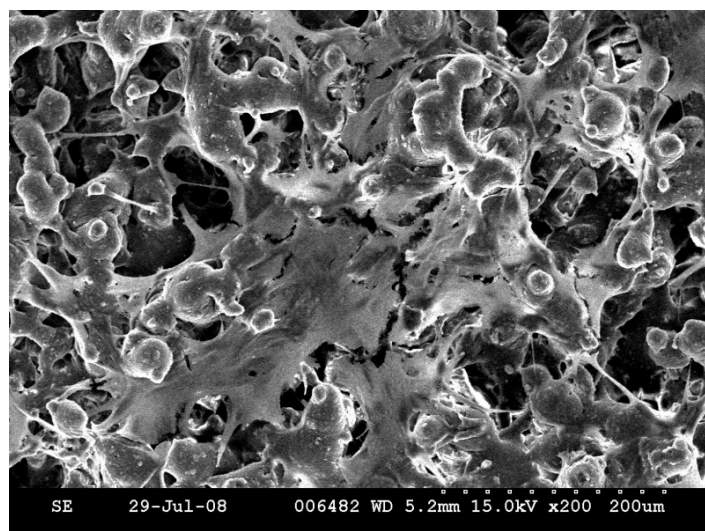


Figure 8. Scanning electron microscopy (SEM) of an attached cell culture. SEM illustrated a high cell confluency of the coated biomaterial and a spreading morphology where cells exhibited extended morphology, which consequently suggested an outstanding degree of the surface biocompatibility.

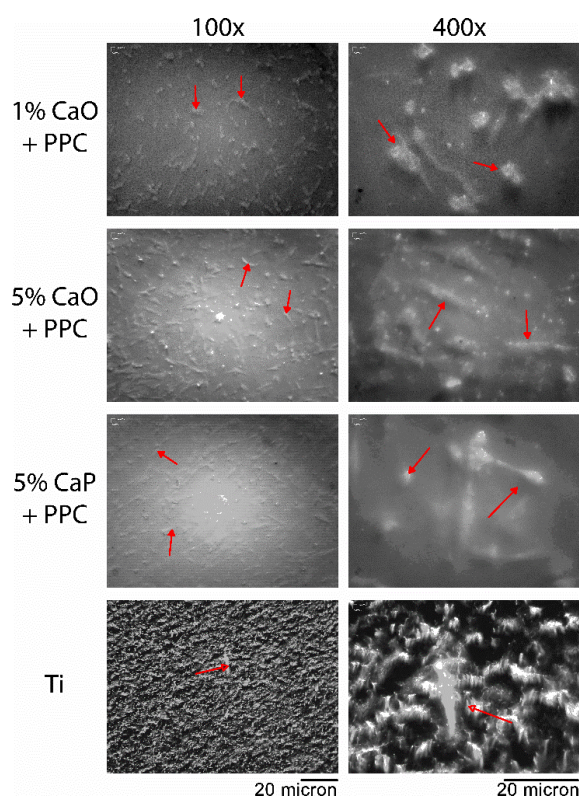


Figure 9. Optical microscopy of the HEPM cell cultures at low (100 \times) and high (400 \times) magnifications. Optical microscopy suggested that all of biomaterials were able to support HEPM cell cultures. However, under lower power (100 \times), the images suggested that the cellular confluence correlated with the incorporation of calcium oxide. While at high magnification (400 \times), a spreading morphology was observed on all of the surfaces, indicating the close association between the cells and their underlying substrate. The arrows are placed to help locate the cells on each surface. (Adapted and modified from [2]).

3.4. Cellular Assays

As previously mentioned, in addition to being biocompatible, a successful orthopedic implant should also possess sufficient osteo-inductivity to ensure proper integration between the implant and surrounding tissue. To study the effects of the coating on the osteo-inductiveness of the substrate, the biomineralization capability of each surface was assessed using Alizarin Red staining. Alizarin Red dyes are known for their ability to bind specifically with mineral deposits through its sulfonic acid and hydroxyl groups; thus, it is often used to label and assess the presence of minerals [39].

The Alizarin Red staining showed that although all of the surfaces were able to demonstrate an increased amount of biomineralization when additional time was allowed for further cellular differentiation and biomineralization, differences were also observed when biomineralization was compared between the various surfaces within the same time group (Figure 10). More specifically, a general trend of increasing mineralization with the increasing level of calcium oxide was observed in both time groups. On the other hand, although the calcium phosphate and the polymer control surfaces also showed increased osteo-inductivity, their efficacies were not nearly as pronounced as calcium oxide. Lastly, the commercially-pure titanium demonstrated the least amount of mineralization in both time groups. The greater extent of biomineralization observed on enriched surfaces could be the result of the calcium functional additive, which could have acted as a seedling for mineralization and thereby increased the accumulation of mineral deposits. The greatest extent of biomineralization observed on calcium oxide surfaces could be explained by the fact that the bioactive additives were incorporated according to their mass percent. Thus, the lower molecular mass of calcium oxide would allow a greater amount of calcium to be incorporated compared to calcium phosphate, resulting in the greatest extent of biomineralization. Similarly, studies have also suggested that the presence of phosphate has been shown to decrease cellular activity, resulting in the reduced biomineralization.

As a result, cellular assays including immunochemistry, optical and SEM microscopy, as well as biomineralization assays were utilized to assess the biological performance of the coated biomaterials. It is evident that while all of the surfaces displayed levels of biocompatibility and osteo-inductivity, the coated surfaces, especially the calcium oxide-containing surfaces demonstrated the greatest level of biocompatibility and osteo-inductivity through their high levels of cell confluency and biomineralization activities. These findings placed calcium oxide-enriched coatings as the better candidate for enhancing orthopedic and bone implants.

Gene expression can be affected by the biocompatibility of the surface which, in turn, can dictate the cellular differentiation and biomineralization activities. To confirm the promising biological responses observed on the by the coated biomaterial surfaces via *in vitro* cellular experiments, quantifiable cellular assays were conducted to study the inductive effects of surface coating on gene expression. Seven different postulated surfaces were compared against the performance of conventional titanium substrate (Table 2). Firstly, the presence of cell cultures observed on coated surfaces during optical and SEM assessments were confirmed using cell counts. During this study, hemocytometry was employed to quantify the surface cellular confluency (Figure 11). The results suggested that the enriched surfaces achieved a similar high cell density as the cultures raised on commercially pure titanium surfaces, indicating the biocompatibility of the coated surfaces.

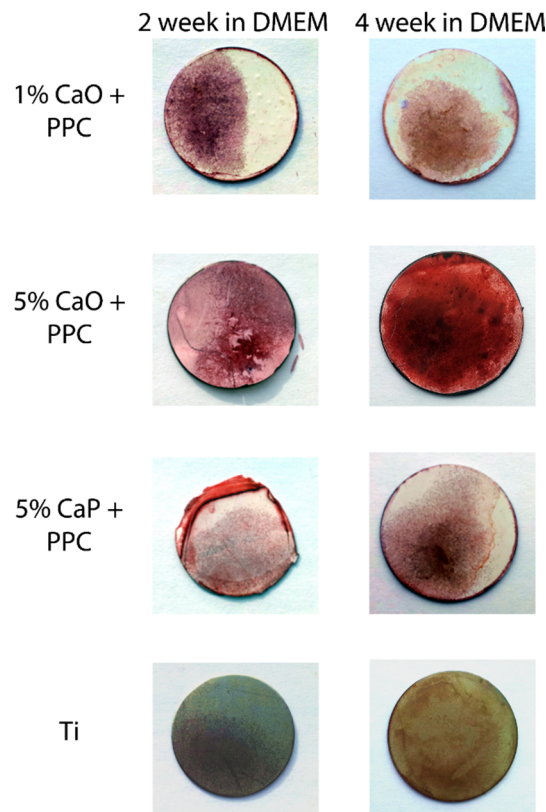


Figure 10. Biomineralization assay using Alizarin Red staining after two weeks and four weeks of proliferation and differentiation. Alizarin Red staining suggested even though all of the surfaces showed increased signs of mineral deposits over time, 5% CaO-containing surfaces exhibited the great degrees of staining after two week and four weeks of proliferation and differentiation. However, conventional titanium showed the least amount of mineral deposits amongst all of the surfaces. (Adapted and modified from [2]).

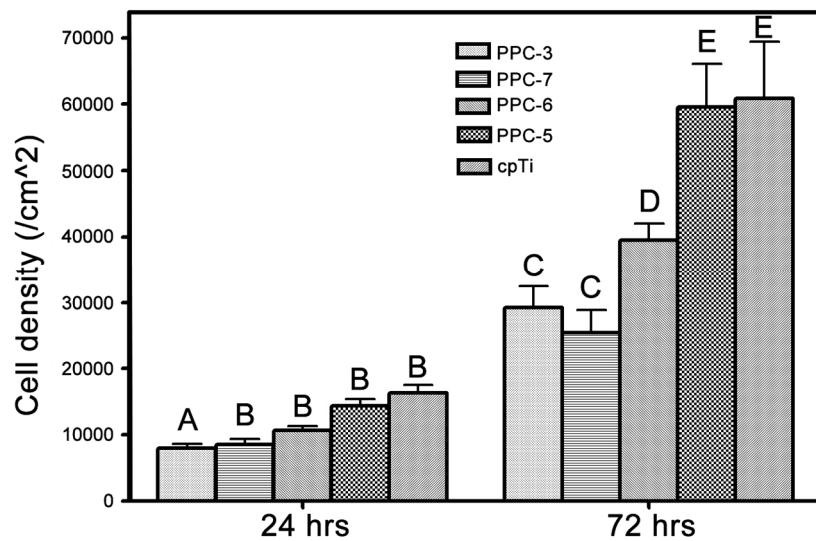


Figure 11. The cellular attachment test after 24 h of incubation and the cellular proliferation study after 72 h of incubation. Hemocytometry suggested that polymer coating could achieve a similar cell confluency as the conventional titanium surfaces. Each letter represents an individual statistical group. (One way ANOVA, $p > 0.05$).

Table 2. Example of coated surface chemical compositions.

Surface	Base	Flow Additive	Embedded TiO ₂ (wt %)	Added nTiO ₂ (wt %)
PPC-1	Epoxy resin + PTFE	nSiO ₂	0	0
PPC-2	Polyester resin + PTFE	nSiO ₂	25.0	0
PPC-3	Polyester resin + PTFE	nTiO ₂	25.0	0.5
PPC-4	Polyester resin + PTFE	nTiO ₂	25.0	2.0
PPC-5	Polyester resin	nTiO ₂	25.0	0.5
PPC-6	Polyester resin + PTFE	nTiO ₂	25.0	0.5
PPC-7	Polyester resin + PTFE	nTiO ₂	25.0	0.5

In addition, effects of the bioactive coatings on cellular metabolic activity, an indicator for biocompatibility, was also quantified using MTT assay. MTT is a colorimetric assay that reveals information regarding the mitochondrial activity; thus, it is often used to assess the cellular metabolic activity. Through MTT assays, a similar trend to hemocytometry was observed (Figure 12). The data suggested that the cell cultures seeded onto enriched surfaces could be equally metabolically active as the commercially-pure titanium cultures. By encouraging the cellular metabolic activities, the attached cultures would have the ability to induce bone formations, which were seen on coated surfaces during earlier Alizarin Red assays. Consequently, to further confirm the osteo-inductivity of the coated biomaterial, the expression of the genes responsible for biomineralization, as well as the constitutional genes that are responsible for the proliferation of the cells were also analyzed using PCR (Figure 13). The results showed that the genes that are essential for cellular survival such as COL1 and GAPDH were observable in all of the cultures; similarly, the bone forming genes such as BSP, RUNX2, and ALP were also expressed in all of the cultures. These results confirmed the viability and the osteogenic differentiation of attached cell culture.

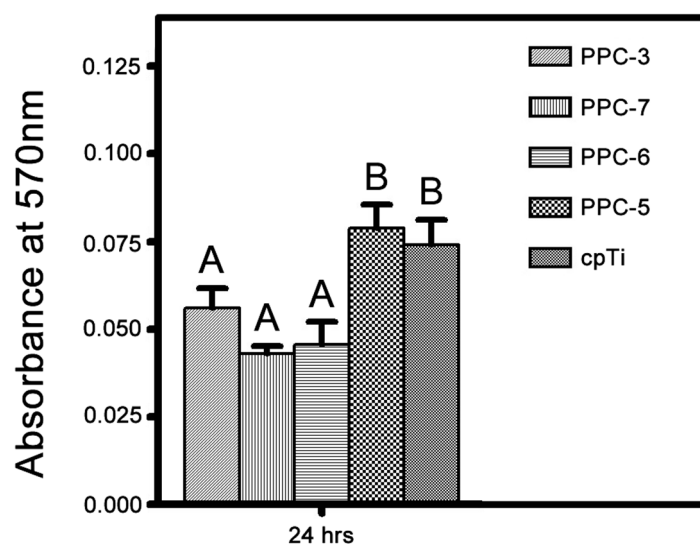


Figure 12. After 24 h of incubation, MTT assay illustrated that the mitochondrial activities varied between surfaces. However, polymer-coated biomaterial could potentially have a higher metabolic activity compared to commercially-pure titanium. Each letter represents an individual statistical group. (One way ANOVA, $p > 0.05$).

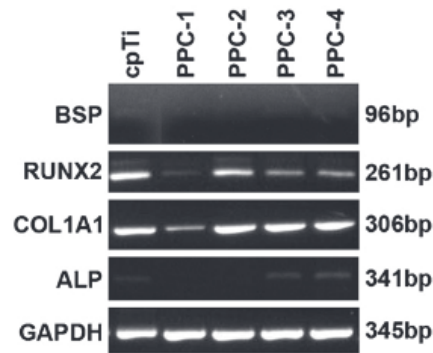


Figure 13. PCR demonstrated all of the constitutional genes, COL1A1, and GAPDH, were expressed by all of the cells. In addition, osteogenic genes and RUNX2 were also expressed to various extents by the cells on different biomaterial surfaces.

In summary, hemocytometry demonstrated that high levels of biocompatibility can be achieved in coated surfaces through, and MTT assays showed that active cells were also found on coated surfaces, which could contribute to the increased biomineralization activity observed in previous studies. Furthermore, PCR also respectively confirmed the biocompatibility and the osteo-inductivity of the polymer based coatings through the high level expressions of the constitutional and osteogenic genes. Thus, the cellular studies showed that not only does the ultrafine particle technology improved the biocompatibility of orthopedic implants, it also effectively increased the osteo-inductivity of conventional implant substrate.

4. Conclusions

Our studies have demonstrated a novel technique which utilized the ultrafine particle technology and bioactive functional additives to effectively improve the biocompatibility and osteo-inductivity of conventional bone implant substrates. This technique can be rapidly and easily applied using the current powder coating instruments. The results suggested that the coated surfaces were able to facilitate cell attachment, exhibit biomineralization, encourage cell proliferation, and increase metabolic activity. Consequently, with future *in vivo* assays, our research team hopes to provide the medical field with a new generation of bone and orthopedic implants that are not only highly biocompatible, but also exhibit outstanding osteo-inductivity to minimize the risk of implant-induced immune responses and create a stronger tissue-implant interface for a better anchorage of the implant.

Conflicts of Interest

The authors declare no conflict of interest.

References

1. Albrektsson, T.; Johansson, C. Osteoinduction, osteoconduction and osseointegration. *Eur. Spine J.* **2001**, *10*, S96–S101.

2. Hou, N.Y.; Zhu, J.; Zhang, H.; Perinpanayagam, H. Ultrafine calcium-titania-polyester dry powder coatings promote human mesenchymal cell attachment and biomineralization. *Surf. Coat. Technol.* **2014**, *251*, 177–185.
3. Shi, W.; Mozumder, M.S.; Zhang, H.; Zhu, J.; Perinpanayagam, H. MTA-enriched nanocomposite TiO₂-polymeric powder coatings support human mesenchymal cell attachment and growth. *Biomed. Mater.* **2012**, *7*, doi:10.1088/1748-6041/7/5/055006.
4. Kim, H.-W.; Kim, H.-E.; Salih, V.; Knowles, J.C. Hydroxyapatite and titania sol-gel composite coatings on titanium for hard tissue implants: Mechanical and *in vitro* biological performance. *J. Biomed. Mater. Res. B Appl. Biomater.* **2005**, *72*, 1–8.
5. Ducheyne, P.; Cuckler, J.M. Bioactive ceramic prosthetic coatings. *Clin. Orthop.* **1992**, *276*, 102–114.
6. Lee, S.-H.; Kim, H.-W.; Lee, E.-J.; Li, L.-H.; Kim, H.-E. Hydroxyapatite-TiO₂ hybrid coating on Ti implants. *J. Biomater. Appl.* **2006**, *20*, 195–208.
7. McPherson, E.J.; Dorr, L.D.; Gruen, T.A.; Saberi, M.T. Hydroxyapatite-coated proximal ingrowth femoral stems. A matched pair control study. *Clin. Orthop.* **1995**, *315*, 223–230.
8. Ramires, P.A.; Romito, A.; Cosentino, F.; Milella, E. The influence of titania/hydroxyapatite composite coatings on *in vitro* osteoblasts behaviour. *Biomaterials* **2001**, *22*, 1467–1474.
9. Gomes, P.S.; Botelho, C.; Lopes, M.A.; Santos, J.D.; Fernandes, M.H. Evaluation of human osteoblastic cell response to plasma-sprayed silicon-substituted hydroxyapatite coatings over titanium substrates. *J. Biomed. Mater. Res. B Appl. Biomater.* **2010**, *94*, 337–346.
10. Nie, X.; Leyland, A.; Matthews, A. Deposition of layered bioceramic hydroxyapatite/TiO₂ coatings on titanium alloys using a hybrid technique of micro-arc oxidation and electrophoresis. *Surf. Coat. Technol.* **2000**, *125*, 407–414.
11. Kasuga, T.; Nogami, M.; Niinomi, M.; Hattori, T. Bioactive calcium phosphate invert glass-ceramic coating on β -type Ti–29Nb–13Ta–4.6Zr alloy. *Biomaterials* **2003**, *24*, 283–290.
12. Anitua, E.; Prado, R.; Orive, G.; Tejero, R. Effects of calcium-modified titanium implant surfaces on platelet activation, clot formation, and osseointegration. *J. Biomed. Mater. Res. A* **2015**, *103*, 969–980.
13. Mendes, V.C.; Moineddin, R.; Davies, J.E. Discrete calcium phosphate nanocrystalline deposition enhances osteoconduction on titanium-based implant surfaces. *J. Biomed. Mater. Res. A* **2009**, *90*, 577–585.
14. Choi, J.-Y.; Jung, U.-W.; Kim, C.-S.; Jung, S.-M.; Lee, I.-S.; Choi, S.-H. Influence of nanocoated calcium phosphate on two different types of implant surfaces in different bone environment: An animal study. *Clin. Oral Implants Res.* **2013**, *24*, 1018–1022.
15. Poulos, N.M.; Rodriguez, N.A.; Lee, J.; Rueggeberg, F.A.; Schupbach, P.; Hall, J.; Susin, C.; Wikesjö, U.M. Evaluation of a novel calcium phosphate-coated titanium porous oxide implant surface: A study in rabbits. *Int. J. Oral Maxillofac. Implants* **2011**, *26*, 731–738.
16. Aniket, A.El-G. Electrophoretic deposition of bioactive silica-calcium phosphate nanocomposite on Ti-6Al-4V orthopedic implant. *J. Biomed. Mater. Res. B Appl. Biomater.* **2011**, *99*, 369–379.
17. De Groot, K.; Geesink, R.; Klein, C.P.A.T.; Serekian, P. Plasma sprayed coatings of hydroxylapatite. *J. Biomed. Mater. Res.* **1987**, *21*, 1375–1381.

18. Vercaigne, S.; Wolke, J.G.C.; Naert, I.; Jansen, J.A. Histomorphometrical and mechanical evaluation of titanium plasma-spray-coated implants placed in the cortical bone of goats. *J. Biomed. Mater. Res.* **1998**, *41*, 41–48.
19. Van Dijk, K.; Schaeken, H.G.; Wolke, J.C.; Marée, C.H.; Habraken, F.H.; Verhoeven, J.; Jansen, J.A. Influence of discharge power level on the properties of hydroxyapatite films deposited on Ti-6Al-4V with RF magnetron sputtering. *J. Biomed. Mater. Res.* **1995**, *29*, 269–276.
20. Yoshinari, M.; Klinge, B.; Dérand, T. The biocompatibility (cell culture and histologic study) of hydroxy-apatite-coated implants created by ion beam dynamic mixing. *Clin. Oral Implants Res.* **1996**, *7*, 96–100.
21. Overgaard, S.; Søballe, K.; Josephsen, K.; Hansen, E.S.; Bünger, C. Role of different loading conditions on resorption of hydroxyapatite coating evaluated by histomorphometric and stereological methods. *J. Orthop. Res.* **1996**, *14*, 888–894.
22. Zhu, J.; Zhang, H. Fluidization Additives to Fine Powders. 2004. Available online: <http://www.google.com/patents?id=SqsQAAAAEBAJ> (accessed on 1 August 2015).
23. Zhang, H.; Zhu, J. Method and Apparatus for Uniformly Dispersing Additive Particles in Fine Powders. U.S. Patent 7,878,430, 1 February 2011.
24. Mozumder, M.S.; Zhu, J.; Perinpanayagam, H. Nano-TiO₂ enriched polymeric powder coatings support human mesenchymal cell attachment and growth. *J. Biomater. Appl.* **2011**, *26*, 173–193.
25. Mozumder, M.S.; Zhu, J.; Perinpanayagam, H. TiO₂-enriched polymeric powder coatings support human mesenchymal cell spreading and osteogenic differentiation. *Biomed. Mater.* **2011**, *6*, doi:10.1088/1748-6041/6/3/035009.
26. Mozumder, M.S.; Zhu, J.; Perinpanayagam, H. Titania-polymeric powder coatings with nano-topography support enhanced human mesenchymal cell responses. *J. Biomed. Mater. Res. A* **2012**, *100*, 2695–2709.
27. Liu, X.; Ma, P.X. Polymeric scaffolds for bone tissue engineering. *Ann. Biomed. Eng.* **2004**, *32*, 477–486.
28. Ma, P.X. Biomimetic materials for tissue engineering. *Emerg. Trends Cell Based Ther.* **2008**, *60*, 184–198.
29. Schneider, G.B.; Zaharias, R.; Seabold, D.; Keller, J.; Stanford, C. Differentiation of preosteoblasts is affected by implant surface microtopographies. *J. Biomed. Mater. Res. A* **2004**, *69*, 462–468.
30. Masaki, C.; Schneider, G.B.; Zaharias, R.; Seabold, D.; Stanford, C. Effects of implant surface microtopography on osteoblast gene expression. *Clin. Oral Implants Res.* **2005**, *16*, 650–656.
31. Ko, Y.J.; Zaharias, R.S.; Seabold, D.A.; Lafoon, J.; Schneider, G.B. Osteoblast differentiation is enhanced in rotary cell culture simulated microgravity environments. *J. Prosthodont.* **2007**, *16*, 431–438.
32. Hallab, N.J.; Bundy, K.J.; O'Connor, K.; Moses, R.L.; Jacobs, J.J. Evaluation of metallic and polymeric biomaterial surface energy and surface roughness characteristics for directed cell adhesion. *Tissue Eng.* **2001**, *7*, 55–71.
33. Rajaraman, R.; Rounds, D.E.; Yen, S.P.S.; Rembaum, A. A scanning electron microscope study of cell adhesion and spreading *in vitro*. *Exp. Cell Res.* **1974**, *88*, 327–339.
34. Deligianni, D.D.; Katsala, N.D.; Koutsoukos, P.G.; Missirlis, Y.F. Effect of surface roughness of hydroxyapatite on human bone marrow cell adhesion, proliferation, differentiation and detachment strength. *Biomaterials* **2000**, *22*, 87–96.

35. Good, R.J. Contact angle, wetting, and adhesion: A critical review. *J. Adhes. Sci. Technol.* **1992**, *6*, 1269–1302.
36. Hu, M.-X.; Yang, Q.; Xu, Z.-K. Enhancing the hydrophilicity of polypropylene microporous membranes by the grafting of 2-hydroxyethyl methacrylate via a synergistic effect of photoinitiators. *J. Membr. Sci.* **2006**, *285*, 196–205.
37. Li, J.; Hastings, G.W. Oxide Bioceramics: Inert ceramic materials in medicine and dentistry. In *Handbook of Biomaterial Properties*; Black, J., Hastings, G., Eds.; Springer: New York, NY, USA, 1998; pp. 340–354.
38. Deligianni, D.; Katsala, N.; Ladas, S.; Sotiropoulou, D.; Amedee, J.; Missirlis, Y. Effect of surface roughness of the titanium alloy Ti–6Al–4V on human bone marrow cell response and on protein adsorption. *Biomaterials* **2001**, *22*, 1241–1251.
39. Puchtler, H.; Meloan, S.N.; Terry, M.S. On the history and mechanism of alizarin and alizarin red s stains for calcium. *J. Histochem. Cytochem.* **1969**, *17*, 110–124.

© 2015 by the authors; licensee MDPI, Basel, Switzerland. This article is an open access article distributed under the terms and conditions of the Creative Commons Attribution license (<http://creativecommons.org/licenses/by/4.0/>).